*Acta Cryst.* (1965). **18**, 678

# Variations in The Structure of Guinier – Preston Zones During Aging*

By Darrell R. James† and Gerald L. Liedl‡

*School of Metallurgical Engineering, Purdue University, Lafayette, Indiana, U.S.A.*

(*Received* 22 *June* 1964)

An analysis of the diffuse scattering from *GP*1 zones in an aluminum − 1·67 at. % copper alloy aged for 6, 12, 24, and 36 hours at 130 °C is given. The diffuse scattering between the 200 and 400 Bragg reflections was measured with a diffractometer employing monochromatic radiation and pulse height discrimination. The diameter of the *GP*1 zones varied from 35 to 63 Å and the copper clustering was contained within 3 to 5 planes. The copper content of the central plane decreased from 57 at. % at 6 hr to 30 at. % at 36 hr. The displacements of the lattice planes from the matrix positions extended beyond 8 planes from the central plane with the maximum displacement at the first plane. The value of the *c* parameter of *GP*2 compared favorably with other investigators. A maximum corresponding to a spacing of 1·27 Å was detected in the diffuse intensity during the formation of *GP*2 and $\theta'$. This maximum was explained as a matching of 6 *GP*2 planes with 5 matrix planes and 8 $\theta'$ planes with 6 matrix planes.

## Introduction

Recent refinements in theoretical methods and experimental techniques (Toman, 1957; Gerold, 1958; Doi, 1960; Thomas, 1961) have allowed investigators to describe more accurately the structure of Guinier–Preston zones in aluminum–copper alloys. These zones, previously named *GP*1, have been described as thin platelets coherent with the (100) matrix planes and varying in diameter from 30–500 Å. Subsequent aging has been shown to produce an ordered coherent structure called *GP*2, a non-equilibrium precipitate $\theta'$, and finally the equilibrium precipitate $\theta$ ($CuAl_2$).

X-ray diffraction data for structure analysis previously have been obtained by film techniques, such as oscillating and precession photographs. These data are difficult to interpret as a result of the non-linear response of the film to the radiation. Consequently, the use of a counter diffractometer with monochromatic radiation and pulse height discrimination should result in more precise data.

Two recent investigations of *GP* zones are those of Doi (1960) and Thomas (1961). In both investigations film methods were used and the amplitude of the scattered radiation was calculated as the positive square root of the corrected intensity. The electron density according to Doi (1960) was calculated by fitting parameters of a model to the data and according to Thomas (1961) by a trial and error method.

The present work followed a similar approach to that of Thomas (1961) and consisted in measuring the diffuse intensity distribution at various aging times for an aluminum-1·67 at.% copper alloy. A diffractometer employing a focusing curved-crystal quartz monochromator, a scintillation counter, and pulse height discrimination was used to record the diffuse intensity. FORTRAN programs developed by the authors for the IBM 7090 computer were employed to correct the observed intensity and to calculate the electron density distribution.

## Theory

It has been shown that for a large number of statistically centrosymmetric zones, the positive square root of the diffuse zone intensity along a line between two Bragg maxima is proportional to the amplitude of scattered radiation (Doi, 1960). Therefore the amplitude distribution is symmetric about the reciprocal origin as is the zone intensity. The operators and functions used in this investigation are defined in Table 1.

Table 1. *Functional definitions*

| | | |
|---|---|---|
| $g(x) \xrightarrow[\cdot]{} G(y)$ | Fourier transform | $G(y)=\int_{-\infty}^{\infty} g(x)\, e^{2\pi i x y} dx$ |
| $H(x)=g(x) * f(x)$ | Convolution product | $H(x)=\int_{-\infty}^{\infty} g(h) f(x-h) dh$ |
| $S(x/a)$ | Truncation function | $S(x/a) \begin{cases} 1, & \lvert x\rvert < a/2 \\ \frac{1}{2}, & \lvert x\rvert = a/2 \\ 0, & \lvert x\rvert > a/2 \end{cases}$ |

If we assume no interaction between the radiation scattered from the zones and the radiation scattered from the matrix, the total intensity may be given as the sum of the intensities. The intensities are the projected intensities as defined by the measuring instrument. Since the intensity of the matrix in the aged condition remains unchanged from the intensity of the matrix in the unaged condition, the zone intensity may be obtained by subtracting the scattered intensity of the specimen in the unaged condition from the intensity

---

* This paper is based upon a thesis submitted by Darrell R. James in partial fulfillment of the degree of M.S.Met.E. at Purdue University in 1964.

† Formerly graduate student at Purdue University, Lafayette, Indiana, and currently 1st Lt. USAF, Wright-Patterson Air Force Base, Ohio, U.S.A.

‡ Assistant Professor of Metallurgical Engineering, Purdue University, Lafayette, Indiana, U.S.A.

scattered from the specimen in the aged condition. If we take the amplitude of scattering between two reciprocal lattice points as the positive square root of the intensity (Doi, 1960), the zone electron density and the amplitude of scattering from the zone, $F(y_1)$, are related by

$$F(y_1) \xrightarrow[\cdot]{} \varrho(x_1)\,. \tag{1}$$

Since it is physically impossible to determine the total amplitude distribution in the $y_1$ direction, a truncation function, $T$, must be introduced to describe the limits of the measurements. In terms of the observed and actual quantities

$$F_{\text{obs}}(y_1) = F_{\text{act}}(y_1) \cdot T(y_1)\,. \tag{2}$$

The Fourier transform of equation (2) yields

$$\varrho_{\text{obs}}(x_1) = \varrho_{\text{act}}(x_1) * t(x_1)\,. \tag{3}$$

The quantities $\varrho_{\text{obs}}(x_1)$ and $t(x_1)$ can be calculated from the observed amplitude and the truncation function. It should be noted that equation (3) is not susceptible to a simple analytical solution for $\varrho_{\text{act}}(x_1)$. Therefore, a relaxation method must be employed to obtain the solution.

Since the Cu atoms substitute for the Al atoms on the Al sites, the shape of the projected electron density in a single layer of the zone will be proportional to the difference in atomic scattering factors of copper and aluminum (Cochran, 1956). The function, $\varrho_{\text{act}}(x_1)$, is synthesized by placing the projected electron-density shape at the assumed position of each plane and weighting this shape by a constant proportional to the at.% Cu in that plane. In this manner adjustments in composition and displacement of the various layers in the zone can be made with each iteration.

## Procedure

The specimen used in this investigation was a flat single crystal (approximately 1 in. diameter and $\frac{3}{16}$ in. thick) of Al-1·67 at.% Cu which was grown by a modified strain anneal method. The crystal was grown with a (100) plane nearly parallel to the specimen surface. The specimen was solution heat treated at 560 °C for 68 hours and quenched in ice water. The diffuse zone intensity was determined between the 200 and 400 reciprocal lattice points by a three-circle diffractometer. A Siemens curved-crystal quartz monochromator set for Cu $K\alpha_1$ radiation was the source. Twelve runs were made at various times between 1 and 300 hours aging at 130 °C. FORTRAN language programs were written for the IBM 7090 computer by the authors to correct the observed intensity and to solve for the actual electron density. This method of data reduction was necessary since approximately 1700 data points were taken for each measurement. The intensity was corrected for Lorentz–polarization, but absorption and Debye thermal scattering were assumed to be negligible in taking the difference in intensities.

Since the amplitude distribution was symmetric, equation (1) was programmed as the cosine transform

$$\varrho_{\text{obs}} = 2\int_{y_a}^{y_b} F_{\text{obs}}(y_1)\cos 2\pi x_1 y_1\, dy_1$$

where $y_a$ and $y_b$ were the $y_1$ coordinate limits of the intensity measurement. The truncation function given by

$$T(y_1) = S(y_1/2y_b) - S(y_1/2y_a)$$

defines the limits of the measurements. The iterative solution of $\varrho_{\text{act}}(x_1)$ was obtained from

$$\varrho_{\text{obs}}(x_1) = \int_c^d \varrho_{\text{act}}(x_1 - x)\,\frac{\sin 2\pi y_b x - \sin 2\pi y_a x}{\pi x}\,dx \tag{4}$$

where $c$ and $d$ were fixed to include the region out to 25 Å from the center of the symmetric zone. An initial assumption for $\varrho_{\text{act}}(x_1)$ was made to evaluate the integral in equation (4). The values of this integral were compared with $\varrho_{\text{obs}}(x_1)$ and appropriate modifications were made in $\varrho_{\text{act}}(x_1)$. Using the modified $\varrho_{\text{act}}(x_1)$, the above procedure was repeated until the evaluation of the integral in equation (4) converged on $\varrho_{\text{obs}}(x_1)$.

The desired solution, $\varrho_{\text{act}}(x_1)$, was determined for *GP*1 for 6, 12, 24, and 36 hours aging at 130 °C. Zone diameters were determined in each run by scanning in reciprocal space perpendicular to the diffuse streak at various positions along the streak. The qualitative aspects of the zone growth were followed to the state of equilibrium precipitation.

## Results and discussion

An example of the general shape of the diffuse scattering from the zone is shown in Fig. 1. For the four runs of 6, 12, 24, and 36 hours aging in which only *GP*1 was present, the displacement and the copper content in each plane of the zone were determined from the solutions of $\varrho_{\text{act}}(x_1)$. These values are given in Table 2. The displacements were determined from the difference between the position of each peak in $\varrho_{\text{act}}(x_1)$ and the corresponding position of the coherent plane in the matrix. The copper content was calculated on the basis that the background is 1·67 at.% Cu and that the areas of each peak are proportional to the square of the copper content (Cochran, 1956). The errors in concentration and displacement were obtained by considering only the fit between the iterative solution in equation (4) and the value of $\varrho_{\text{obs}}(x_1)$ calculated from the amplitude distribution. Consequently, the actual errors are probably larger.

The results given in Table 2 are not in agreement with either Doi (1960) or Thomas (1961) for 36 hours aging. In particular, the gradient of the copper concentration as determined in this investigation is smaller, and the strain field exists beyond 8 layers instead of the previously reported 2 layers. In Fig. 1, it is apparent that a major contribution to the zone intensity occurs

Table 2. *GP*1 *zone structure between* 6 *and* 36 *hours*

| | Plane | 6 hr | 12 hr | 24 hr | 36 hr |
|---|---|---|---|---|---|
| | Center | 57 | 45 | 47 | 30 |
| Copper | 1 | 2·8 | 2·6 | 3 | 2·2 |
| content | 2 | 1·67 | 2·1 | 2·1 | 1·67 |
| at. % | 3 | 1·67 | 1·67 | 1·67 | 1·2 |
| (±5 % of value) | 4 | 1·67 | 1·67 | 1·67 | 1·67 |
| Displacement | 1 | 22·5 | 22·5 | 22·5 | 22·5 |
| toward | 2 | 12·5 | 12·5 | 12·5 | 12·5 |
| origin | 3 | 12·5 | 12·5 | 12·5 | 12·5 |
| x $10^{+2}$ Å | 4 | 12·5 | 12·5 | 12·5 | 12·5 |
| (±0·025 Å) | 5 | 12·5 | 10 | 10 | 10 |
| | 6 | 10 | 10 | 7·5 | 7·5 |
| | 7 | 10 | 7·5 | 7·5 | 7·5 |
| | 8 | 10 | 7·5 | 7·5 | 7·5 |
| Zone diameter Å (±10 Å) | | 35 | 48 | 56 | 63 |

very close to the 200 Al reflection. Since the zone intensity determined by Thomas (1961) and the intensity used by Doi (1960) were obtained by film methods, the accuracy of the difference in film blackening near the Bragg peak for long exposures is subject to large errors. Calculations of the electron-density distribution for changes in the shape and height of this peak in the diffuse streak indicate that there is a major effect on the results. The authors are, therefore, of the opinion that the major difference in these investigations is related to the accuracy in the diffuse intensity near the Bragg peak. Since counter methods are inherently more accurate in intensity measurements, the authors are of the opinion that the results of the present investigation are more realistic. A comparison of the results of this investigation with both Doi (1960) and Thomas (1961) is shown in Fig. 2.

After 36 hours aging, a maximum in the diffuse streak at point *A* in Fig. 1 corresponding to *GP*2 (Silcock, 1953) was detected. Continued aging intensified this maximum and resulted in a shift of position to a higher Bragg angle. Table 3 gives the change in *c*-spacing of *GP*2 calculated from the observed maximum.

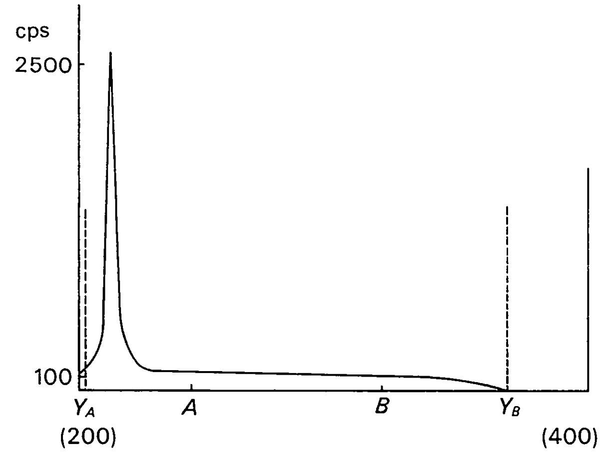

Fig. 1. General shape of diffuse zone intensity after correction for Lorentz-polarization.

Table 3. *Change of c-spacing of GP*2 *with aging*

| Aging time at 130°C | c spacing of GP2, Å (±0·01 Å) | Zone Diameter, Å (±10 Å) |
|---|---|---|
| 72 hr | 7·9 | 86 |
| 108 | 7·73 | 112 |
| 168 | 7·68 | 132 |
| 188 | 7·66 | 143 |
| 224 | 7·65 | 147 |
| 275 | 7·63 | 147 |

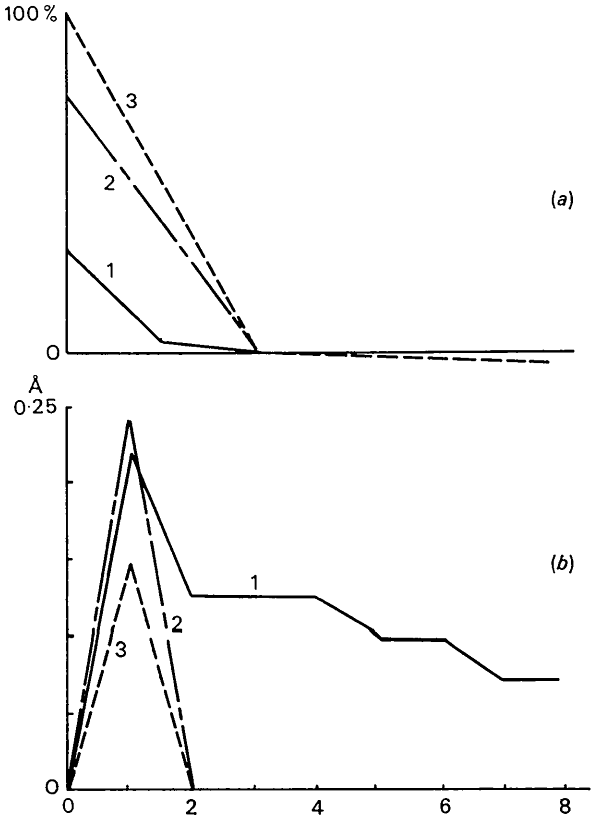

Fig. 2. The results of structure analyses of present authors (curves 1), by Thomas (curves 2) and by Doi (curves 3). (*a*) The atomic composition of Cu in each plane. (*b*) The displacement of each plane toward the zone origin. The abscissa is expressed in units of $\frac{1}{2}a_0$.

The first non-coherent precipitate, $\theta'$, was detected after 303 hours at 130 °C plus 24 hours at 200 °C. On the basis of the (004) $\theta'$ reflection measured in this work, the $c$ parameter of $\theta'$ is $5{\cdot}84 \pm 0{\cdot}01$ Å.

During the growth of $GP2$ a diffuse maximum existed at an angle which corresponded to plane spacings of 1·27 Å ($B$ in Fig. 1). This maximum became very weak after the formation of $\theta'$ and was completely absent after the equilibrium $CuAl_2$ was formed. Diffuse maxima have been reported in $\theta'$ before (Guinier, 1942), and the present authors propose the following explanation based on the results of this work. Based on the 1·27 Å spacing, the diffuse maximum observed during $GP2$ growth can be explained by a coherent 'matching' of 6 $GP2$ planes and 5 matrix planes (*i.e.* a 6th order reflection from a pseudo-lattice of 10·1 Å spacing). The diffuse maximum during $\theta'$ growth is explained by a similar coincidence of 8 $\theta'$ planes with 6 matrix planes (8th order reflection). The above configurations were chosen since they represent the lowest possible coherency strains between the existing $GP$ structure and the matrix.

The sequence of transformation is seen to be gradual and tends toward a state of lower strain energy. As shown in Table 2, the copper content during the formation of $GP1$ gradually decreases to the approximate equilibrium composition as the diameter of the zone increases. At this stage an ordering of the Cu atoms takes place along with an increase in size of the zone and produces enough lattice misfit to form a non-coherent configuration.

The authors wish to acknowledge the Air Force Institute of Technology and the Advanced Research Projects Agency, Department of Defense, Contract SD-102, for their support of this investigation.

## References

Cochran, W. (1956). *Acta Cryst.* **9**, 259.
Doi, K. (1960). *Acta Cryst.* **13**, 45.
Gerold, V. (1958). *Acta Cryst.* **11**, 230.
Guinier, A. (1942). *J. Phys. Radium,* **3**, 124.
Silcock, J. (1953). *J. Inst. Metals,* **82**, 239.
Thomas, A. D. (1961). Ph. D. Thesis, Purdue University, Lafayette, Indiana.
Toman, K. (1957). *Acta Cryst.* **10**, 187

---

*Acta Cryst.* (1965). **18**, 681

# A Three-Dimensional Analysis of Instrumental Broadening in X-Ray Measurements

By Gerald L. Liedl* and Pekka Rautala†

*Purdue University, Lafayette, Indiana, U.S.A.*

(*Received* 22 *June* 1964)

The effects of the source distribution, divergence slits, Soller slits, source width at the specimen, and absorption were interpreted as a three-dimensional measuring function in reciprocal space. The analysis of these instrumental effects was calculated for a particular set of instrumental coordinates chosen to minimize the number of instrumental effects along the paths of measurements.

The effect of the measuring functions for monochromatic radiation along the coordinates chosen was shown for cleaved single crystals of calcite and zinc. The measurements verify the proposed analysis and illustrate the three-dimensional character of the measurements.

## Introduction

The experimental conditions of any diffraction experiment require finite source and receiving openings which result in divergent beams. Consequently, the conditions for diffraction may be fulfilled over a range of angles defined in part by these openings, *i.e.* by the instrument. The region in reciprocal space which does give rise to scattering is restricted by both the instrument and the specimen. The instrument defines the maximum possible region while the specimen may restrict the active region to some smaller portion of the maximum region.

The region defined by the instrument is three-dimensional, and for any real specimen, the active region defined by the specimen is also three-dimensional. Therefore, any diffraction measurement is inherently a three-dimensional measurement of the scattered intensity over a finite region, *i.e.* a power. The authors feel strongly that this three-dimensional nature of the measurements must be considered in the interpretation of the diffraction effects.

The elimination of instrumental effects in diffraction studies has been confined mainly to a one-dimensional analysis. The early work of Spencer (1931, 1939,

---

* Assistant Professor of Metallurgical Engineering, Purdue University, Lafayette, Indiana, U.S.A.

† Formerly Professor at Purdue University, Lafayette, Indiana. Present address: Tapiola, Finland.